LA-10268-MS

C.3

*Preliminary Study of
Uranium Oxide Dissolution in
Simulated Lung Fluid*

Los Alamos
Los Alamos National Laboratory
Los Alamos, New Mexico 87545

Prepared by Helen L. York, Group HSE-5

Preliminary Study of
Uranium Oxide Dissolution in
Simulated Lung Fluid

R. C. Scripsick
K. C. Crist*
M. I. Tillery
S. C. Soderholm
S. J. Rothenberg**

*Conoco, Inc., Ponca City, Oklahoma.
**Lovelace Inhalation Toxicology Research Institute, Lovelace Biomedical and Environmental
Research Institute, P. O. Box 5890, Albuquerque, NM 87185.

REPORT DOCUMENTATION PAGE		READ INSTRUCTIONS BEFORE COMPLETING FORM
1. REPORT NUMBER AFATL-TR-84-27	2. GOVT ACCESSION NO.	3. RECIPIENT'S CATALOG NUMBER
4. TITLE *(and Subtitle)* Preliminary Study of Uranium Oxide Dissolution in Simulated Lung Fluid		5. TYPE OF REPORT & PERIOD COVERED Final Report 27 Nov 81 - 30 Sep 83
		6. PERFORMING ORG. REPORT NUMBER LA-10268-MS
7. AUTHOR(s) R. C. Scripsick S. C. Soderholm K. C. Crist S. J. Rothenberg M. I. Tillery		8. CONTRACT OR GRANT NUMBER(s) Project Order ATL-2-296
9. PERFORMING ORGANIZATION NAME AND ADDRESS Los Alamos National Laboratory P. O. Box 1663 Los Alamos, NM 87545		10. PROGRAM ELEMENT, PROJECT, TASK AREA & WORK UNIT NUMBERS Program Element 28030F JON: 2708GC03
11. CONTROLLING OFFICE NAME AND ADDRESS AFATL/DLOE Eglin, AFB, FL 32542		12. REPORT DATE January 1985
		13. NUMBER OF PAGES 25
14. MONITORING AGENCY NAME & ADDRESS*(if different from Controlling Office)*		15. SECURITY CLASS. *(of this report)* Unclassified
		15a. DECLASSIFICATION/DOWNGRADING SCHEDULE N/A

16. DISTRIBUTION STATEMENT *(of this Report)*

Approved for Public Sale - Distribution Unlimited

17. DISTRIBUTION STATEMENT *(of the abstract entered in Block 20, if different from Report)*

18. SUPPLEMENTARY NOTES

19. KEY WORDS *(Continue on reverse side if necessary and identify by block number)*

Uranium, Depleted Uranium, Physicochemical Character of Uranium, Uranium Aerosols, Dissolution Analysis

20. ABSTRACT *(Continue on reverse side if necessary and identify by block number)*

Depleted uranium oxide aerosols prepared in the laboratory and collected in the field were tested to characterize their dissolution in simulated lung fluid and to determine how dissolution is affected by aerosol preparation histories. Respirable fraction samples of each study material were subjected to in vitro dissolution analysis.

Particular trends regarding the physicochemical character of uranium oxides described by other investigators were supported by the data generated in this study. The data suggest that under some conditions a rapidly dissolving uranium fraction may be formed concurrent with the production of UO_2. This fraction may play an important role in determining the hazard potential associated with inhalation exposure to certain uranium aerosols.

DD FORM 1473   EDITION OF 1 NOV 65 IS OBSOLETE
1 JAN 73

CONTENTS

TABLES

FIGURES

PRELIMINARY STUDY OF URANIUM OXIDE DISSOLUTION IN SIMULATED LUNG FLUID[*]

by

R. C. Scripsick, K. C. Crist, M. I. Tillery,
S. C. Soderholm, and S. J. Rothenberg

ABSTRACT

Depleted uranium oxide aerosols prepared in the laboratory and collected in the field were tested to characterize their dissolution in simulated lung fluid and to determine how dissolution is affected by aerosol preparation histories. Respirable fraction samples of each study material were subjected to <u>in vitro</u> dissolution analysis.

Particular trends regarding the physicochemical character of uranium oxides described by other investigators were supported by the data generated in this study. The data suggest that under some conditions a rapidly dissolving uranium fraction may be formed concurrent with the production of UO_2. This fraction may play an important role in determining the hazard potential associated with inhalation exposure to certain uranium aerosols.

I. INTRODUCTION

Depleted uranium (DU), a by-product of the uranium fuel cycle,[1] has been selected by the US military for use in several types of munitions.[2] During development, manufacture, testing, deployment, and use of these munitions,

---

opportunities exist for inhalation exposure to various (usually oxide) aerosol forms of DU.[2] The release of respirable aerosol material from test firings and burning of DU penetrators has been demonstrated.[3-7] Inhalation exposures during the manufacture of the munitions have been reported.[8]

The hazard potential associated with such exposures is closely related to the dynamic partitioning of the DU material deposited in lung. Material retained in lung tissue presents a hazard because of the radiation dose to lung.[9] As material is transported to blood, the primary hazard shifts to chemical kidney damage.[9]

In general, the physicochemical form of the exposure material affects the partitioning of deposited material.[10] Aerodynamic aerosol size determines lung deposition pattern. Material deposited in different regions of the lung is cleared by different paths, rates, and mechanisms. Three lung clearance pathways have been defined: (1) transport to lymph node, (2) transport to gastrointestinal tract, and (3) transport directly to blood. The fraction of deposited material cleared by each of these pathways is dependent on the in vivo dissolution behavior of the deposited material.[10] Consequently, the aerosol size and the dissolution behavior are the important variables in describing the partitioning of deposited material.

Mercer[11] has derived a theoretical relation between dissolution behavior and chemical form and specific surface area (Sp) of a lognormal distribution of particles. He found that the mass fraction remaining $(M(t)/M_0)$ at time t (for $M(t)/M_0 > \sim 0.2$) can be approximated by

$$M(t)/M_0 = \exp(-\lambda t) , \qquad\qquad (1)$$

where

$M(t)$ = mass remaining at time t;

M_0 = mass at initial time t_0;

λ = 1.18 $Sp_0 \cdot k$, which is the long-term dissolution rate constant derived by Mercer;[11]

k = the chemical dissolution rate constant; and

Sp_0 = specific surface area at t = 0.

Several investigators have experimentally studied the dissolution behavior of uranium material under conditions simulating the dissolution environment of

the lung.[12-18] Of these studies, all those that displayed dissolution data as a function of time[14-18] showed phased-dissolution behavior; that is, dissolution starts with a relatively rapid initial dissolution phase followed by a long-term dissolution phase, which is characterized by a slower dissolution rate. The initial dissolution phase may include more than one dissolution component, each having a characteristic rate, the slowest of which is greater than the long-term dissolution rate.

In one study[16] of uranium "yellow cake," Eidson attributed the initial dissolution phase to the ammonium diuranate component of the yellow cake. Follow-up animal inhalation studies,[19] using the same yellow-cake study material, support this contention and, along with human excretion data cited by Eidson,[16] demonstrate the ability of in vitro dissolution analysis to predict in vivo dissolution.

Some of the more recent studies[15,16,18] have described this dissolution behavior by a sum of exponential terms of the form

$$M(t)/M_0 = \sum_{i=1}^{n} f_i \cdot \exp(-\lambda_i t) , \tag{2}$$

where f_i is the fraction of the material associated with dissolution component i and dissolving with dissolution rate constant λ_i, and n is the number of dissolution components. The dissolution half-times, $T_i = (\ln 2)/\lambda_i$, for the initial dissolution phase varied from a fraction of a day to ~12 days. The long-term phase varied from 40 days to ~800 days. In a study of uranium oxide aerosols produced during test firing of DU penetrators,[6] as much as 49 per cent of the uranium material dissolved in the initial dissolution phase.

In this investigation, DU material prepared from DU penetrators oxidized under various controlled conditions in the laboratory and material collected in the field from test firings of. DU penetrators were studied using in vitro dissolution analysis techniques. In addition, the sample material was analyzed for uranium compounds using x-ray diffraction, and the Sp of certain study material was measured before and after dissolution. These data were interpreted to describe the dissolution behavior of these materials and to relate this behavior to certain physical parameters of the study materials.

Inferences regarding the hazard potential associated with inhalation of the study materials are made from the data.

II. MATERIALS AND METHODS

A. Study Materials

Five DU study materials produced in the laboratory were examined by exposing uranium alloy penetrators to certain controlled oxidation atmospheres.[7] In addition, two DU study materials collected from an enclosed test bunker were provided by the United States Air Force (USAF). Table I gives a description of each of the study materials.

The five laboratory study materials were produced from XM774-type antitank munitions penetrators. The penetrators are machined from DU metal alloy containing 0.75 wt% titanium.[20] Oxidation of the penetrators took place in a tube furnace that permitted the control of temperature, atmosphere composition, and gas flow. The conditions under which oxidation took place are detailed in Table I. Material that fell off or could be brushed off the penetrators after the oxidation treatment was collected and comprises the laboratory study materials.

The two bunker study materials were collected by the USAF at an enclosed test bunker used for test firings of various DU penetrator munitions (Table I). One study material (S682-2) was collected as a core sample of the bunker material; the other (S682-1) was collected by the bunker air-cleaning system. These materials were described by the USAF as containing ~10 and ~20 wt% uranium, respectively. The magnitude of these uranium concentrations is supported by duplicate chemical analyses performed at Los Alamos. The major component of the bunker study materials was found to be SiO_2.

TABLE I

DEPLETED-URANIUM STUDY MATERIALS

Study Material No.	Treatment
A774-2	600°C with airflow
A774-4	700°C with airflow
A774-5	900°C with airflow
M774-1	500°C with CO_2/airflow
N774-1	700°C without airflow
S682-2	Bunker core sample
S682-1	Bunker air sample

B. Sample Generation

Each study material was generated as an aerosol, and a respirable size fraction of the aerosol was collected (Fig. 1). Before aerosol generation, the bulk study material was sieved, and the portion passing a 400-mesh (38-μm mesh size) screen was collected. We pressed an aliquot of the sieved material into a specially made thimble, taking care not to disturb the particle size of the sample. The packed thimble was mounted on a Wright dust feed[21] that was used to generate aerosol. The dust feed operates by rotating a sample plug against a radially positioned blade that is continually swept by a jet of clean air, which suspends the material scraped from the plug. The output of this generator was conducted to a horizontal elutriator operated to pass an aerosol that meets the British Medical Research Council criterion[22] as the respirable fraction of the challenge aerosol. Sets of samples representing each study material were collected on 25-mm-diam (5-μm pore size) Millipore membrane filters.

C. Dissolution Analysis

Before subjecting the respirable fraction samples to dissolution analysis, we determined the mass of uranium (M_0) on each filter using a gross gamma radiometric technique. The technique uses a NaI scintillation detector to measure the gamma activity associated with the sample. Standards to relate activity to M_0 were prepared using the laboratory study materials.

Once M_0 was determined, the filter containing the respirable fraction uranium sample was sandwiched between two 25-mm-diam (0.1-μm pore size) Nucleopore membrane filters and placed in a dissolution chamber. The chamber (Fig. 2) used was a one-sided flow system described by Allen[17] and designed by Moss.[23]
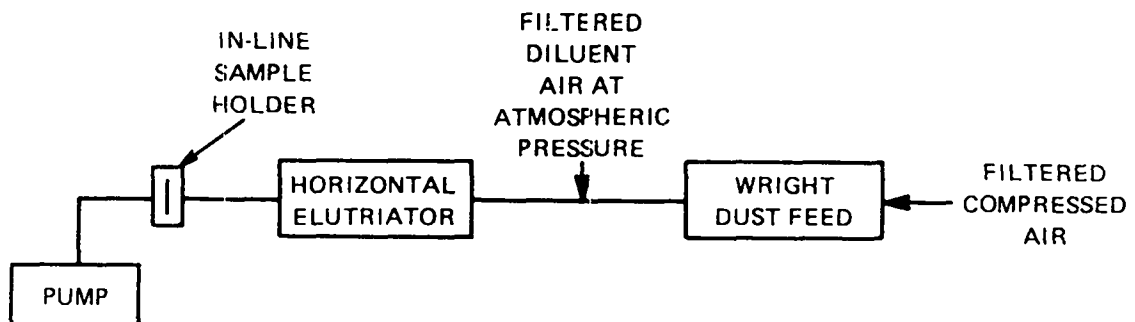
Fig. 1. Respirable aerosol generation system.
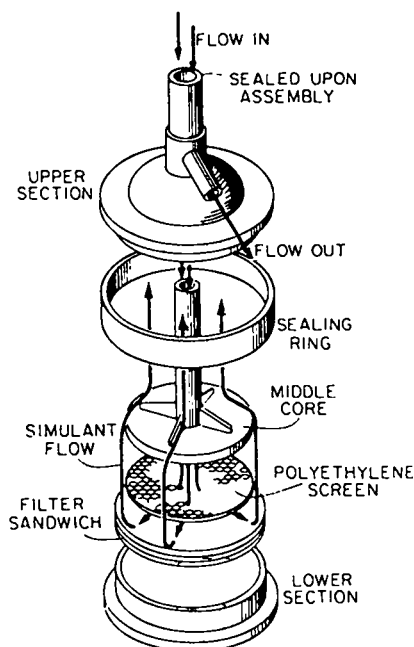
Fig. 2. The dissolution chamber.

The solvent used in the study was a lung-fluid simulant described by Moss.[24] The components of the solution are shown in Table II. A comparison completed by Kalkwarf[15] showed that the simulant and the lung interstitial fluid are almost identical. The protein components in actual lung fluid were represented by equivalent amounts of citrate as suggested by Moss.[24] The lung-fluid simulant was prepared in 156-L batches using deionized water. To

TABLE II

COMPONENTS OF THE SIMULATED LUNG SOLUTION

Component	Concentration (g/L)
Magnesium chloride, hexahydrate	0.203
Sodium chloride	6.019
Potassium chloride	0.298
Sodium phosphate, dibasic, anhydrous	0.142
Sodium sulfate, anhydrous	0.071
Calcium chloride, dihydrate	0.368
Sodium acetate, trihydrate	0.953
Sodium bicarbonate	2.604
Sodium citrate, dihydrate	0.097

increase the rate of solution, 95 per cent of the final volume of water was preheated to 37°C. The salts were separately premixed using the remainder of the water volume to aid in their dissolution. The salt solutions were then transferred to the preheated water in the order listed in Table II. During this procedure, the pH of the solution would increase (pH 8-9), causing a precipitate. This precipitate formation was controlled by lowering the pH to approximately 7 with dilute HCL.

The lung-fluid simulant was delivered to the dissolution chamber by a peristaltic pump at a flow rate of ~1 mL/min. According to Allen,[17] if the rate of flow through the dissolution chamber is kept above 0.7 mL/min, then dissolution rate will be independent of the flow rate. The pH of the simulant was maintained at 7.4 ± 0.1 by slowly bubbling 95 per cent O_2 and 5 per cent CO_2 through the simulant, as suggested by Moss.[24] The temperature of the simulant was maintained at 37°C ± 0.5°C in a water bath. The pH and temperature of the simulant were monitored during the experiments, which were operated for at least 30 days.

Simulant passing out of the dissolution chamber was sampled at known times. The samples were collected in polyethylene bags, which were heat sealed and placed in pneumatic "rabbits" for delayed-neutron activation (DNA) analysis. This DNA technique was selected over fluorometric methods normally used in uranium dissolution studies because (1) the simpler sample handling reduced potential errors in sample analysis, (2) the automated system at Los Alamos permitted the analysis of many more samples for a given effort, and (3) the sensitivity of the DNA technique allowed direct measurement of the dissolved uranium.

Standards for the DNA analysis were prepared using National Bureau of Standards uranium standard reference material 950a, which is natural-abundance U_3O_8. The difference in ^{235}U abundance between the standard material and the study materials was accounted for in the calculation of uranium mass from DNA results.

Blank samples (samples with no added uranium) for the DNA analysis were obtained using a dissolution sandwich containing a middle filter on which no uranium material had been collected. Dissolution of this sandwich was carried out simultaneously with the dissolution of the respirable-fraction samples using simulant from the same reservoir. These samples were collected and analyzed in the same manner as the samples from the other dissolution system.

7

D. X-ray Diffraction Analysis

The composition of bulk and respirable fraction samples was determined using x-ray diffraction. The method, which followed the procedure outlined by Klug,[25] used a standard vertical diffractometer with a graphite monochrometer and a proportional detector. This technique permits the determination of species and quantity of crystalline materials and can detect the presence of amorphous materials at levels >10-20 wt%. To ascertain the percentage of uranium oxide present as the dioxide, standards were prepared from well-characterized, selected UO_2 and U_3O_8 powders. A calibration curve was then drawn from which the results were obtained. The analysis was performed by the Physical Metallurgy Group at Los Alamos.

E. Specific Surface Area Analysis

The Sp of certain respirable fraction samples was measured using a [85]Kr radiometric technique developed by Rothenberg.[26] This technique compares the amount of radioactivity adsorbed on a sample with the amount adsorbed on a sample of standard Sp material. The analysis was performed at Lovelace Inhalation Toxicology Research Institute. The samples selected for Sp analysis included respirable fraction samples of study materials A774-4 and M774-1 and others of these same samples that had undergone dissolution analysis.

III. DATA ANALYSIS AND RESULTS

From the DNA data and values of M_0, estimates of the fraction of remaining uranium dissolved per day (f_d) were calculated as follows:

$$f_{d,j} = \frac{m_j}{d \cdot \left[M_0 - \sum_{k=1}^{j} \left(\frac{(m_k + m_{k-1}) \cdot (t_k - t_{k-1})}{2 \cdot d} \right) \right]} \tag{3}$$

where

m_j and m_k = the mass of uranium in the jth and kth samples, respectively;

t_k = elapsed time, in days, to the midpoint of the sample collection period; and

d = duration of sample collection, in days.

8

The results of these calculations were plotted against time for each of the study materials. Curves were fit to these data using a nonlinear least-squares fitting routine[27] with the variance of each f_d value weighting the fit. The plots with the fitted curves are shown in Figs. 3-6. These plots demonstrate the multiple phase behavior described earlier. These data were fit with a model of the form

$$f_d = \frac{M(t - d/2) - M(t + d/2)}{d \cdot M(t)} . \tag{4}$$

Substituting for M(t) from Eq. 2 yields

$$f_d = \sum_{i=1}^{n} \frac{[\sinh(d\lambda_i) \cdot f_i \cdot \exp(-\lambda_i t)]}{d \cdot [\sum_{i=1}^{n} f_i \cdot \exp(-\lambda_i t)]} , \tag{5}$$

where n is the number of dissolution components included in the fit.

The fitting routine would not converge for n > 2 even though a three-component (n = 3) fit seemed appropriate from inspection of the plots. Fitting of all the data in any given data set with n = 2 resulted in large systematic residuals between data points predicted from the fitted curve and actual data points. A large negative bias was displayed by each of the data sets in the region corresponding to the first of the three observed dissolution components. Consequently, data corresponding to the latter two of the three observed dissolution components were fit with n = 2, which resulted in improved fits to the data including substantial reduction of the large systematic bias. The values of the regression coefficients for these fits are listed in Table III. Characterization of the earliest observed dissolution component was limited to estimates of f_1 (see Table III) and a lower limit on λ_1. The value of λ_2 was used as the lower limit of λ_1.

For sufficiently large t, f_d becomes time independent and takes on the value of λ_3. Conservative estimates were made when the contribution of the first two dissolution components to the overall dissolution rate became insignificant. The average value of f_d corresponding to times beyond this
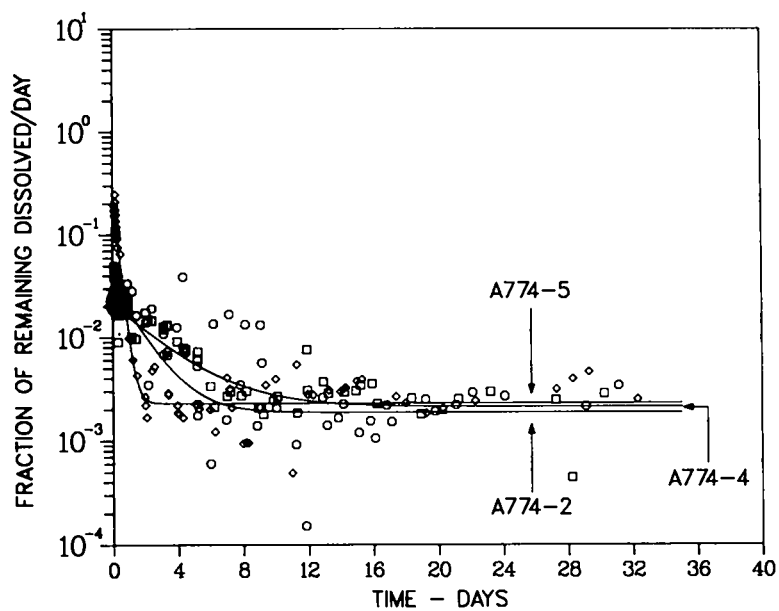
Fig. 3. Plot of data and fitted curves for materials
A774-2(○), A774-4 (□), and A774-5 (◇).

Fig. 4. Plot of data and fitted curves for material M774-1.
The data are from two dissolution experiments, each
using a respirable fraction sample of material M774-1.
The curves coincide in the long term.

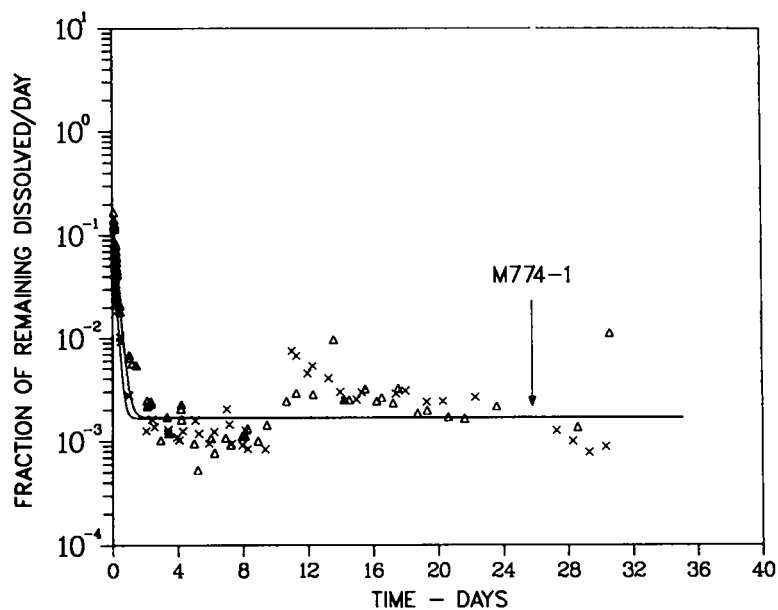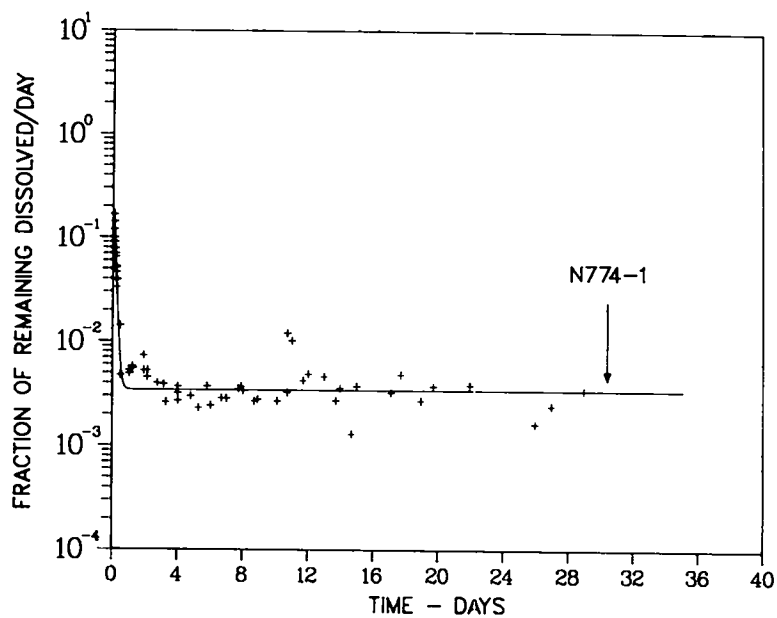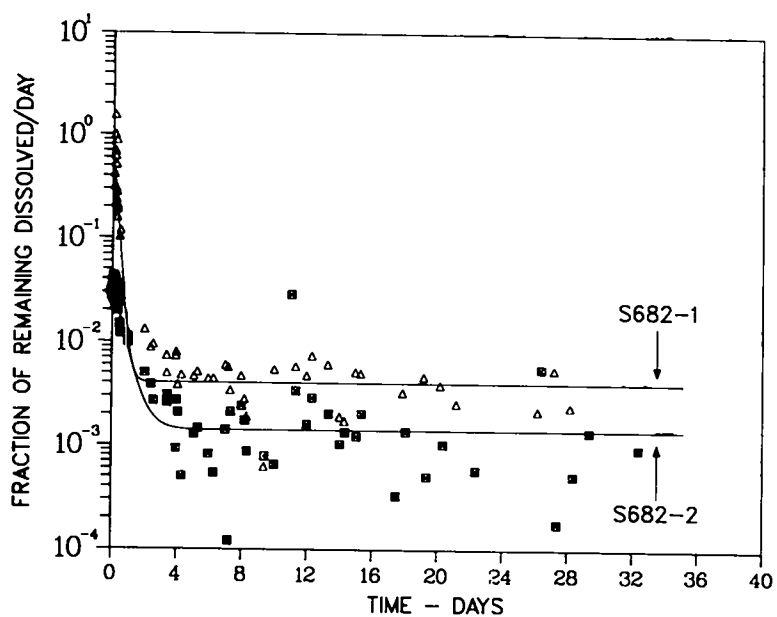Fig. 5. Plot of data and fitted curve for material N774-1.

Fig. 6. Plot of data and fitted curves for the bunker study
materials S682-2 (⊗) and S682-1 (△).

TABLE III

DISSOLUTION PARAMETERS DERIVED FROM EXPONENTIAL LEAST-SQUARES FITS

| Study Material No. | N^a | Initial Dissolution Phase | | | | Long-Term Dissolution Phase | | |
| | | First Component | Second Component | | | Third Component | | |
		f_1	f_2	λ_2 $(days^{-1})$	T_2 $(days)$	f_3	λ_3 $(days^{-1})$	T_3 $(days)$
A774-2	73	0.02 ± 0.001^b	0.05 ± 0.006	0.65 ± 0.1	1.1 ± 0.2	0.94 ± 0.006	$1.9 \times 10^{-3} \pm 3.8 \times 10^{-4}$	370 ± 70
A774-4	71	0.01 ± 0.0008	0.05 ± 0.007	0.35 ± 0.04	2.0 ± 0.03	0.94 ± 0.007	$2.1 \times 10^{-3} \pm 3.8 \times 10^{-4}$	320 ± 60
A774-5	61	0.03 ± 0.003	0.07 ± 0.003	3.5 ± 0.2	0.20 ± 0.01	0.90 ± 0.004	$2.3 \times 10^{-3} \pm 1.6 \times 10^{-4}$	300 ± 20
M774-1	61	0.04 ± 0.002	0.04 ± 0.002	4.8 ± 0.5	0.14 ± 0.01	0.92 ± 0.003	$1.7 \times 10^{-3} \pm 1.5 \times 10^{-4}$	410 ± 40
M774-1	55	0.05 ± 0.003	0.02 ± 0.002	6.6 ± 0.8	0.10 ± 0.01	0.93 ± 0.003	$1.7 \times 10^{-3} \pm 1.6 \times 10^{-4}$	420 ± 40
N774-1	60	0.05 ± 0.002	0.04 ± 0.003	9.6 ± 0.8	0.07 ± 0.006	0.92 ± 0.002	$3.4 \times 10^{-3} \pm 1.9 \times 10^{-4}$	202 ± 10
S682-2	61	0.02 ± 0.0006	0.02 ± 0.002	1.7 ± 0.2	0.41 ± 0.06	0.95 ± 0.002	$1.4 \times 10^{-3} \pm 2.0 \times 10^{-4}$	490 ± 70
S682-1	56	0.12 ± 0.04	0.13 ± 0.01	4.7 ± 0.5	0.14 ± 0.02	0.75 ± 0.03	$4.0 \times 10^{-3} \pm 4.7 \times 10^{-4}$	170 ± 20

[a]Number of data points associated with the analysis.
[b]Value ± standard deviation.

point was computed as an estimate of λ_3. This value of λ_3 was considered to be free of influence from earlier f_d values that affect the estimation of λ_3 by the least-squares method mentioned above. Table IV gives the values of λ_3 obtained by this analytical method. Multiple-comparisons analysis performed using these results indicated a significant difference (at the 95 per cent confidence interval) between the λ_3 values associated with study materials S682-2 and S682-1 and between the values associated with study materials A774-2 and N774-1.

The results of x-ray diffraction analysis of the bulk and respirable fraction samples indicated that the crystalline uranium in the samples was U_3O_8 and UO_2. Table V shows the percentage of the sample that was UO_2; the balance of the crystalline uranium material was U_3O_8. Amorphous material was detected in the respirable fraction sample of the bunker air sample material (S682-1). The fraction of the sample associated with amorphous material was estimated to be ~20 wt%.

Results of the Sp analysis are displayed in Table VI. The Sp associated with the samples ranged from 0.64 m^2/g to 3.85 m^2/g. For both study materials, the Sp of the post-dissolution samples was lower than the Sp of the pre-dissolution samples. The average fractional decrease in Sp was 52 per cent.

TABLE IV

LONG-TERM PHASE DISSOLUTION PARAMETERS CALCULATED USING
AVERAGING TECHNIQUE

Study Material No.	N^a	λ_3 (Days^{-1})	T_3 (Days)
A774-2	16	$2.1 \times 10^{-3} \pm 2 \times 10^{-4}$ [b]	330 ± 30
A774-4	15	$2.6 \times 10^{-3} \pm 2 \times 10^{-4}$	260 ± 20
A774-5	18	$3.0 \times 10^{-3} \pm 3 \times 10^{-4}$	230 ± 20
M774-1[c]	22	$2.9 \times 10^{-3} \pm 5 \times 10^{-4}$	240 ± 45
N774-1	27	$3.8 \times 10^{-3} \pm 4 \times 10^{-4}$	180 ± 21
S682-2	22	$1.5 \times 10^{-3} \pm 3 \times 10^{-4}$	480 ± 85
S682-1	25	$3.8 \times 10^{-3} \pm 4 \times 10^{-4}$	180 ± 20

[a]Number of data points associated with analysis.
[b]Value ± standard deviation.
[c]Only one of the replicate sets of data for this material was analyzed by this technique.

TABLE V

RESULTS OF X-RAY DIFFRACTION ANALYSIS

Study Material No.	UO_2 (wt% in sample)[a]	
	Respirable Fraction	Bulk
A774-2	<0.2[b]	0.6
A774-4	<0.2	1.6
A774-5	1.3	18[b]
M774-1	<0.2	<0.2
N774-1	0.2	6
S682-2	54	97
S682-1	18	60

[a]Remainders are U_3O_8.
[b]The error in this estimate is <±20 per cent of this value. The error in the other estimates is <±10 per cent of the respective values.

TABLE VI

RESULTS OF SPECIFIC SURFACE AREA (Sp) ANALYSIS

Study Material No.	Specific Surface Area		Decrease (%)
	Pre-Dissolution (m^2/g)	Post-Dissolution (m^2/g)	
A774-4	1.84[a]	0.64	65
M774-1	3.85	2.36	39

[a]Error in Sp estimate is <±5 per cent of the respective value.

IV. DISCUSSION AND CONCLUSIONS

In all of the previously cited uranium dissolution studies, an initial dissolution phase was evident.[13,14,6,15,16,18] Review of Steckle's studies[13] of laboratory-produced mixtures of U_3O_8 and UO_2 and Kalkwarf's study[15] of U_3O_8 "pure reference material" show that, at most, only a few per cent of the material dissolve in the initial phase. The respirable fraction of the laboratory study materials examined had between 6

and 10 per cent of the material dominating dissolution during the initial phase. Only ~4 per cent of the respirable fraction of the bunker core sample material (S682-2) was associated with initial phase dissolution. The respirable fraction of the bunker air-sample material (S682-1) studied and similar samples studied by Glissmeyer[6] had from 11 to 49 per cent of the material associated with initial phase dissolution. These data suggest that a larger fraction of material suspended during DU penetrator test firings may be readily available for systemic contamination than would be indicated by the clearance classifications of U_3O_8 and UO_2 [10,14,15] or the results of in vitro studies of laboratory-prepared U_3O_8 and UO_2 material.[13,15]

The initial phase dissolution rates observed in this study ranged from less than 0.07 days to 2 days. These rates are of such a magnitude that if they were observed in vivo as clearance rates from lung to blood, this clearance pathway would compete with other clearance pathways for material deposited in lung. This competition would result in a larger portion of the deposited material being transported from lung to blood than would be expected for class "Y" materials. In addition, clearance of material from lung to blood at such rates could result in accumulation of material in organs such as kidney that have slower clearance rates to urine (kidney half-time clearance to urine is six days or greater) than the rate at which material would be transported to blood.

The long-term dissolution half-times observed here (from 180 days to 480 days) fall in the range of long-term half-times found by Eidson[16] for similar materials (from 140 days to 500 days). These half-times also agree with the "Y" clearance classifications assigned to U_3O_8 and UO_2.[10,14,15]

The range of long-term dissolution half-times relating to long-term lung clearance half-times may not be sufficiently large to warrant the assignment of the long-term component to different hazard classifications. For example, the long-term components would qualify for a "Y" classification under the Task Group on Lung Dynamics classification scheme.[10] However, the range of material fractions dissolving in the initial dissolution phase is probably large enough to warrant assigning significantly different hazard potentials to the various study materials for many exposure scenarios.

The trend of uranium-to-oxygen ratio increasing with preparation temperature described by Steckle[13] and Elder[7] was corroborated by the

results of the x-ray diffraction analysis on both bulk and respirable fraction of the laboratory study materials. The increased UO_2 content in material, prepared under no-gas-flow conditions (N774-1) with respect to material produced in airflow (A774-4) reported by Elder,[7] was also observed.

A significant difference in the UO_2 content between bulk and respirable fraction samples was observed in all study materials. Glissmeyer[6] noticed a similar size segregation. The direction of this segregation, namely, that U_3O_8 is associated with the smaller particle sizes, agrees with data presented by Steckle[13] and Elder.[7]

This finding points out the importance of performing dissolution analysis and other analyses on appropriate size-selected samples. Analysis of bulk material or even total particulate samples may result in inaccurate predictions of lung clearance rates and/or incorrect associations between dissolution half-times and physicochemical character of study material. These inaccurate predictions and incorrect associations, in addition to being related to differences in the physical character of deposited and study materials, may also be related to chemical differences in these materials.

The bunker study materials (S682-2 and S682-1) had a higher UO_2 content than did the laboratory materials. A relatively high UO_2 content was also evident in the material studied by Glissmeyer.[6] In light of the thermal history effect on composition described above, the elevated UO_2 levels indicate that the bunker study materials may have been produced at higher temperatures than were the laboratory samples. The higher UO_2 content may also have been a result of rapid quenching of the material after heating.

Eidson[16] attributed the initial phase seen in the dissolution of yellow-cake samples to the presence of ammonium diuranate, a rapidly dissolving uranium material. The relatively large amount of material dissolved in the initial dissolution phase of bunker air sample material (S682-1) may be related to the production of a rapidly dissolving fraction in the test firing of penetrators. Because the rapidly dissolving fraction was observed to a lesser degree in the bunker core sample material (S682-2), the fraction may include particles with relatively low settling velocities, which as a consequence for a given specific gravity, would have a relatively high Sp. The fact that ~20 wt% of the respirable fraction sample of study material S682-1 was found to be amorphous and that this amorphous material may contain uranium suggests that at least a portion of the rapidly dissolving

16

fraction may be rapidly dissolving amorphous uranium compounds. Therefore, rather than chemical character of the material alone accounting for initial phase dissolution as Eidson found for yellow cake, initial phase dissolution for material S682-1 may be a consequence of the physical character of the material as well as of the chemical composition of the material.

The initial dissolution phase observed for the bunker core sample material (S682-2) and the laboratory study materials may also result from the physical and chemical character of these study materials. Pre- and post-dissolution Sp analysis of the respirable fraction of two laboratory study materials (A774-4 and M774-1) showed Sp at the end of the dissolution experiment to be lower than the initial Sp of the materials. Such behavior is predicted for single-component materials, which are lognormally distributed in diameter with geometric standard deviations greater than ~1.135 (see Appendix). However, the multiple-phase dissolution behavior observed here indicates that the materials studied were not single-component. Decrease in Sp of multiple-component material is possibly the result of relatively rapid dissolution of one or more of the material components that have relative high Sp. The rapid dissolution would be the result of the high Sp and also possibly the presence in the component of rapidly dissolving amorphous or crystalline uranium compounds that exist at concentrations below the detection limit of the x-ray diffraction technique used.

An additional important factor is the change of surface roughness with time. Thibault[28] demonstrated that even carefully polished metal surfaces are not perfectly smooth. He was able to show a correlation between initial dissolution rates and the surface roughness of materials cut from a single block and polished or machined by different methods. After a few days, the prominences and channels produced by most mechanical treatments had disappeared, and both the surface roughness and dissolution rates tended to have common values, independent of the method of polishing. Because the particles produced by combustion are not smooth spheres, the surface roughness may decrease as dissolution proceeds, with prominences on the particle suffering rapid initial attack.

The long-term dissolution half-time associated with the respirable fraction of study material S682-1 (bunker air sample) was significantly higher (at the 95 per cent confidence level) than was the long-term dissolution half-time associated with the respirable fraction of study material S682-2

(bunker core sample). Because the major difference between these materials may be the result of elutriation, study material S682-1 may consist of particles with lower settling velocities than study material S682-2. Consequently, for a given specific gravity, the Sp of study material S682-1 would be greater than the Sp of material S682-2. This greater Sp could at least partially account for the difference observed in the long-term dissolution half-times associated with the respirable fraction of these study materials.

The long-term dissolution half-time associated with respirable fraction of study material A774-2 was significantly higher (at the 95 per cent confidence level) than was the long-term half-time associated with the respirable fraction material N774-1. This difference is in conflict with the trend of preparation temperature and "solubility" described by Steckle[13] and Cooke.[14] The conflict may be because the temperature range for which the Steckle and Cooke trend is described is greater than the range of temperatures studied here. The long-term half-time difference seen in this study may be related to the different airflow conditions under which materials were produced. As mentioned earlier, the no-airflow condition seems to produce material with a relatively greater UO_2 abundance. A relatively high UO_2 abundance was also noticed in the bunker air sample material (S682-1) that was associated with a relatively low, long-term dissolution half-time. This finding suggests that there may be some relation between the depression of U_3O_8 production and the long-term dissolution half-time.

Another partial explanation for the conflict may involve the variety of crystalline phases and the range of stoichiometries associated with each phase possible for uranium oxides between UO_2 and UO_3. Each of these phases, and perhaps the different stoichiometries within a phase, may dissolve at different rates.

V. SUMMARY

The amount of material dissolving in the initial dissolution phase and the rate at which material dissolved in this phase were the determining factors in assessing the hazard potential associated with sample materials. The "Y" clearance classification normally associated with U_3O_8 and UO_2 does not adequately describe the clearance of deposited material indicated by in vitro dissolution analysis. This discrepancy is especially true for the bunker air

sample material (S682-1) of which ~25 per cent dissolved with a half-time ≤ 6 h.

The size segregation of composition between bulk and respirable samples points out a potential pitfall in the evaluation of the dissolution of U_3O_8 and UO_2. Study of size fractions other than that which deposits in the lungs can lead to incorrect conclusions regarding the effects of the material's physical and chemical characteristics upon dissolution.

APPENDIX

DERIVATION OF SPECIFIC SURFACE AREA BEHAVIOR AS A FUNCTION OF TIME: AUGMENTING MERCER'S CALCULATIONS

According to Mercer,[11] the rate at which the mass of a particle dissolves is given by

$$d(m)/dt = -ks \quad , \tag{A-1}$$

where m = the mass of the particle at time t, and s = the surface area of the particle at time t. Using the relationships

$$m = \alpha_v \rho D^3 \tag{A-2}$$

and

$$s = \alpha_s D^2 \quad , \tag{A-3}$$

where

α_v = the diameter volume-shape factor,

α_s = the diameter surface-shape factor,

ρ = the specific gravity of the material being dissolved, and

D = the particle diameter at time t.

Integrating, we find that

$$s = s_0[1 - (k\alpha_s t/3\alpha_v \rho D_0)]^2 \quad , \tag{A-4}$$

where s_0 = s at $t = 0$, and D_0 = D at $t = 0$.

For a lognormal distribution of aerosol particles having a mass median diameter D_m and geometric standard deviation σ_g at $t = 0$, the total surface area remaining after dissolving for a time t, $S(t)$, is given by

$$S(t) = [S_0/\sigma(2\pi)^{1/2}] \int_{X_t}^{\infty} (s/s_0)\exp - [(X-X_m + \sigma^2)^2/2\sigma^2]dX \quad , \tag{A-5}$$

20

where

S_0 = the total surface area at $t = 0$,

σ = $\ln\sigma_g$,

X = $\ln D_0$,

X_m = $\ln(D_m)$,

X_t = $\ln D_t$, and

D_t = the diameter of the particles that completely dissolve in time
$\quad$ t.

The relation between the surface median diameter D_s and the mass median diameter has been used: $D_s = D_m e^{-2}$. Substituting with Eq. A-4 and expanding yields

$$S/S_0 = \sum_{i=0}^{2} K_i \int_{y_i}^{\infty} f(y)dy \quad , \tag{A-6}$$

where

$f(y) = (2\pi)^{-1/2}\exp(-y^2/2)$, $K_0 = 1$, $K_1 = -(2/3)\beta\exp(1.5\sigma^2)$,

$K_2 = \beta^2\exp(4\sigma^2)/9$, $\beta = \alpha_s kt/\alpha_v\rho D_m$, and

$y_i = (\ln(\beta/3)/\sigma) + (1+i)\sigma$.

S/S_0 is shown in Fig. A-1 as a function of β for $\sigma = 0.85$. Also shown in Fig. A-1 is M/M_0 and $Sp/Sp_0 = (S/S_0)/(M/M_0)$ for $\sigma = 0.85$. M/M_0 was calculated according to Mercer.[11]

In Fig. A-2, Sp/Sp_0 is plotted as a function of β for $\sigma = 0$, 0.1, 0.3, 0.5, and 0.85. For $\sigma <$ ~0.028, Sp/Sp_0 increases uniformly, with Sp/Sp_0 going to infinity at $\beta = 3$. For ~0.028 $< \sigma <$ ~0.13, Sp/Sp_0 increases to a maximum and then decreases, but never goes below 1. For ~0.13 $< \sigma <$ ~0.49, Sp/Sp_0 increases to a maximum and then decreases below 1. Finally, for $\sigma >$ ~0.49, Sp/Sp_0 decreases uniformly.
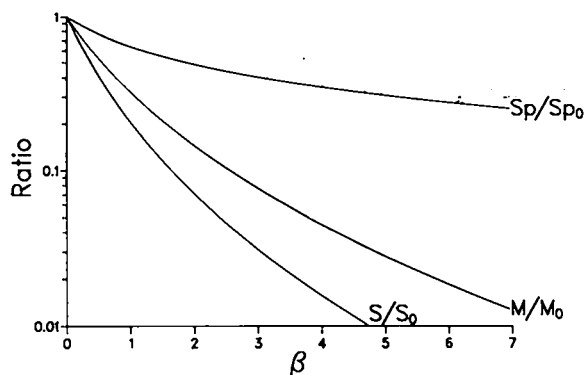
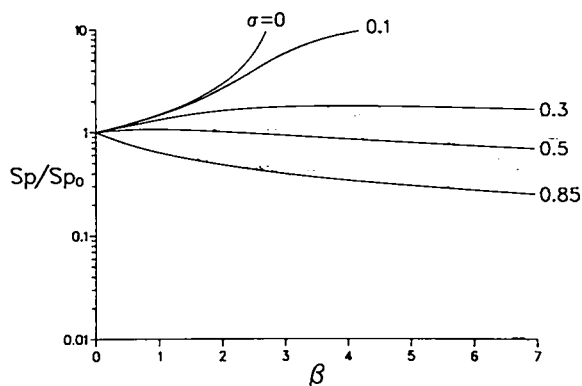Fig. A-1. Plot of S/S_0, M/M_0, and Sp/Sp_0 as a function of β for $\sigma = 0.85$.

Fig. A-2. Plot of Sp/Sp_0 as a function of β for $\sigma = 0$, 0.1, 0.3, 0.5, and 0.85.

REFERENCES

1. S. Gladstone, "Energy Deskbook," Department of Energy report DOE/IR/05114-1 (June 1982).

2. R. L. Gilchrist, "The Safe Use of Depleted Uranium in Munitions," Health Physics 38, 1010-1011 (1980).

3. W. C. Hanson, J. C. Elder, H. J. Ettinger, L. W. Hantel, and J. W. Owen, "Particle Size Distribution of Fragments from Depleted Uranium Penetrators Fired Against Armor Plate Targets," Los Alamos Scientific Laboratory report LA-5654 (October 1974).

4. J. C. Elder, M. I. Tillery, and H. J. Ettinger, "Hazard Classification Test of GAU-8 Ammunition by Bonfire Cookoff with Limited Air Sampling," Los Alamos Scientific Laboratory report LA-6210-MS (February 1976).

5. J. C. Elder, M. I. Tillery, and H. J. ittinger, "Hazard Classification Test of Mixed-Load 30mm GAU-8 Ammunition by Bonfire Cookoff and Sympathetic Detonation Testing," Los Alamos Scientific Laboratory report LA-6711-MS (February 1977).

6. J. A. Glissmeyer and J. Mishima, "Characterization of Airborne Uranium from Test Firings of XM774 Ammunition," Pacific Northwest Laboratory report PNL-2944 (1979).

7. J. C. Elder and M. C. Tinkle, "Oxidation of Depleted Uranium Penetrators and Aerosol Dispersal at High Temperatures," Los Alamos Scientific Laboratory report LA-8610-MS (December 1980).

8. S. Carpnell, "Radioactive Dust Fuels a Bitter 10-month Strike," Occupational Hazards 44, 99-103 (1982).

9. International Commission on Radiological Protection, "Report of Committee IV on Evaluation of Radiation Doses to Body Tissues from Internal Contamination due to Occupational Exposure," ICRP Publication 10 (Pergamon Press, Oxford, 1966).

10. Task Group on Lung Dynamics, "Deposition and Retention Models for Internal Dosimetry of the Human Respiratory Tract," Health Physics 12, 173-207 (1966).

11. T. T. Mercer, "On the Role of Particle Size in the Dissolution of Lung Burdens", Health Physics 13, 1211-122] (1967).

12. P. E. Morrow, F. R. Gibb, and L. Johnson, "Clearance of Insoluble Dust from the Lower Respiratory Tract," Health Physics 10, 543-555 (1964).

13. L. M. Steckle, C. M. West, "Characterization of Y-12 Uranium Process Materials Correlated with In Vivo Experience," US Atomic Energy Commission report Y-1544-A (1966).

14. N. Cooke and F. B. Hold, "The Solubility of Some Uranium Compounds in Simulated Lung Fluid," Health Physics 27. 69-77 (1974).

15. D. R. Kalkwarf, "Solubility Classification of Airborne Uranium Products from LWR-Fuel Plants," Pacific Northwest Laboratory report PNL-3411 (1980).

16. A. F. Eidson and J. A. Mewhinney, "In vitro Solubility of Yellow-Cake Samples from Four Uranium Mills and the Implications for Bioassay Interpretation," Health Physics 39, 893-902 (1980).

17. M. D. Allen, J. K. Briant, O. R. Moss, E. J. Rossignol, D. D. Mahbum, L. G. Morgan, J. L. Ryan, and R. P. Turcotte, "Dissolution Characteristics of LMFBR Fuel-Sodium Aerosols," Health Physics 40, 183 (1981).

18. N. A. Dennis, H. M. Blauer, and J. E. Kent, "Dissolution Fractions and Half Times of Single Source Yellowcake in Simulated Lung Fluids," Health Physics 42, 469-477 (1982).

19. E. G. Damon, A. F. Eidson, F. F. Hahn, A. C. Griffith, Jr., and R. A. Guilmatte, "Comparison of Early Lung Clearance of Yellow Cake in Rats with In Vitro Dissolution and IR Analysis," Health Physics 46, 859-866 (1984).

20. W. T. Barlett, R. L. Gilchrist, W. A. Endres, and J. L. Baer, "Radiation Characterization, and Exposure Rate Measurements from Cartridge 105-mm, APFSDS-T, XM774," Pacific Northwest Laboratory report PNL-2947 (1979).

21. B. M. Wright, "A New-Feed Mechanism," Journal of Scientific Instruments 27, 12 (1975).

22. Aerosol Technology Committee, "Guide for Respirable Mass Sampling," American Industrial Hygienists Association Journal 33, 133 (1970).

23. O. R. Moss, and G. M. Kanapilly, "Dissolution of Inhaled Aerosols," in Generation of Aerosols, Klaus Willeke, Ed. (Ann Arbor Science, Ann Arbor, Michigan, 1980).

24. O. R. Moss, "Simulants of Lung Interstitial Fluid," Health Physics 36, 447 (1979).

25. H. P. Klug and L. E. Alexander, X-Ray Diffraction Procedures (Wiley, New York, 1974).

26. S. J. Rothenberg, P. B. Denee, Y. S. Cheng, R. L. Hanson, H. C. Yeh, and A. F. Eidson, "Methods for the Measurement of surface Areas of Aerosols by Adsorption," Advances in Colloid and Interface Science 15, 223-249 (1982).

27. J. H. Trussel, "Generalized Least Square Package," Los Alamos Program Library Write-up, GFAA, Los Alamos National Laboratory (1979).

28. S. Thibault, J. M. Godot, J. Pagetti, and J. Talbot, "Exemples de l'Influence de l'Etat de Surface des Metaux sur leur Aptitude a la Corrosion et sur l'Action de Inhibiteurs," in "Proceedings of the 4th International Congress on Metal Corrosion, National Association of Corrosion Engineering" (1969).

EXTERNAL DISTRIBUTION

	No. of Copies		No. of Copies
DTIC-DDAC Cameron Station Alexandria, VA 22314	2	HQ PACAF/DOOQ Hickam AFB, HI 96861	2
AUL-LSE Maxwell AFB, AL 36112	1	TAC/INAT Langley AFB, VA 23665	1
ASD/ENSZ (Mr. W. E. Hartley) Wright-Patterson AFB, OH 45433	1	ASD/XRX Wright-Patterson AFB, OH 45433	1

AFATL/DLODL
Eglin AFB, FL   32542
	2	US Army TRADOC Systems
		  Analysis ACTY/ATTA-SL
		  (Library)
		White Sands Missile Range,
		NM 88002
			1

AFATL/CC Eglin AFB, FL 32542	1		
HQ USAF/SAMI Washington, DC 20330	1	COMIPAC/PT-2 Box 38 Camp H.M. Smith, HI 96861	1
OO-ALC/MMWMC Hill AFB, UT 84406	1	HQ PACAF/OA Hickam AFB, HI 96853	1
HQ AFIS/INT Washington, DC 20332	2	USA Ballistics Research Laboratory ARRADCOM/DRDAR-TSB-S Aberdeen Proving Ground, MD 21005	1
ASD/ENESS (Uncl. Only) Wright-Patterson AFB, OH 45433	1		
HQ TAC/DRA Langley AFB, VA 23665	1	AFATL/CCN	1
		AFATL/DLODA	1
HQ USAFE/DOQ APO New York 09012	1	FTD/SDNF Wright-Patterson AFB, OH 45433	1

Los Alamos